

Recent Test Results of the High Field Nb₃Sn Dipole Magnet HD2

P. Ferracin, B. Bingham, S. Caspi, D. W. Cheng, D. R. Dietderich, H. Felice, A. R. Hafalia, C. R. Hannaford, J. Joseph, A. F. Lietzke, J. Lizarazo, G. Sabbi, X. Wang

Accelerator Fusion Research Division
Ernest Orlando Lawrence Berkeley National Laboratory
University of California
Berkeley, California 94720

DISCLAIMER

This document was prepared as an account of work sponsored by the United States Government. While this document is believed to contain correct information, neither the United States Government nor any agency thereof, nor The Regents of the University of California, nor any of their employees, makes any warranty, express or implied, or assumes any legal responsibility for the accuracy, completeness, or usefulness of any information, apparatus, product, or process disclosed, or represents that its use would not infringe privately owned rights. Reference herein to any specific commercial product, process, or service by its trade name, trademark, manufacturer, or otherwise, does not necessarily constitute or imply its endorsement, recommendation, or favoring by the United States Government or any agency thereof, or The Regents of the University of California. The views and opinions of authors expressed herein do not necessarily state or reflect those of the United States Government or any agency thereof or The Regents of the University of California.

This work was supported by the Director, Office of Science, Office of Fusion Energy Sciences, of the U.S. Department of Energy under Contract No. DE-AC02-05CH11231.

Recent Test Results of the High Field Nb₃Sn Dipole Magnet HD2

P. Ferracin, B. Bingham, S. Caspi, D. W. Cheng, D. R. Dietderich, H. Felice, A. R. Hafalia, C. R. Hannaford, J. Joseph, A. F. Lietzke, J. Lizarazo, G. Sabbi, and X. Wang

Abstract—The 1 m long Nb₃Sn dipole magnet HD2, fabricated and tested at Lawrence Berkeley National Laboratory, represents a step towards the development of block-type accelerator quality magnets operating in the range of 13–15 T. The magnet design features two coil modules composed of two layers wound around a titanium-alloy pole. The layer 1 pole includes a round cutout to provide room for a bore tube with a clear aperture of 36 mm. After a first series of tests where HD2 reached a maximum bore field of 13.8 T, corresponding to an estimated peak field on the conductor of 14.5 T, the magnet was disassembled and reloaded without the bore tube and with a clear aperture increased to 43 mm. We describe in this paper the magnet training observed in two consecutive tests after the removal of the bore tube, with a comparison of the quench performance with respect to the previous tests. An analysis of the voltage signals recorded before and after training quenches is then presented and discussed, and the results of coil visual inspections are reported.

Index Terms—Dipole magnet, Nb₃Sn.

I. INTRODUCTION

IN 2008, the LBNL Superconducting Magnet Program tested the Nb₃Sn dipole magnet HD2. The magnet design is characterized by a shell-based support structure, similar to the one used for the previous high field dipole HD1 [1], which provides pre-load and support to a two-layer block-type coil. The coil was assembled around a stainless steel tube which provided support to pole and windings during the pre-loading operations and featured a clear aperture of 36 mm. HD2 was tested three times, as HD2a-b-c, and the test results, including preliminary field quality measurements, were reported in [2]–[4]. During the HD2c test, the magnet started training at about 70% of the expected maximum current I_{SS} , and, after 30 quenches, reached a maximum bore field of 13.8 T (87% of I_{SS}), corresponding to an estimated peak field on the conductor of 14.5 T. After the test, the magnet was unloaded, disassembled, and reassembled without the bore tube. The removal of the bore was aimed at improving the vertical support of the coil, and, at the same time, increasing the magnet clear aperture to 43 mm. Following the re-loading operations, two additional tests were performed (HD2d-e).

Manuscript received October 20, 2009. First published March 29, 2010; current version published May 28, 2010. This work was supported by the Director, Office of Energy Research, Office of High Energy and Nuclear Physics, High Energy Physics Division, US Department of Energy, under Contract DE-AC02-05CH11231.

The authors are with Lawrence Berkeley National Laboratory, Berkeley, CA 94720 USA (e-mail: pferracin@lbl.gov).

Color versions of one or more of the figures in this paper are available online at <http://ieeexplore.ieee.org>.

Digital Object Identifier 10.1109/TASC.2010.2042046

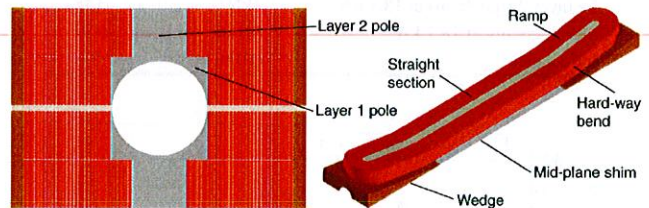


Fig. 1. Coil cross-section (left) and 3D design (right).

We describe in this paper the quench performance of the HD2 magnet assembled without the bore tube. After a brief description of coil design and magnet parameters (we refer to [5]–[7] for the support structure design), the paper focuses on loading sequence and effect of bore removal on coil stresses. Then, we address training performance and quench locations, and identify possible quench triggering mechanisms pointed out by voltage signals and coil visual inspections.

II. COIL DESIGN AND MAGNET PARAMETERS

The HD2 coils, whose cross-section and 3D design are shown in Fig. 1, are composed of two layers wound with a 51 strands cable. Layer 1, with 24 turns, is wound around a titanium alloy pole, characterized by a round cutout with a clear aperture of 43 mm in diameter. In the original design, the aperture was 36 mm because of the presence of a stainless steel tube which provided additional support to the layer 1 pole. Layer 2, with 30 turns, is wound around another solid titanium alloy pole. The two coils, separated by a stainless steel mid-plane shim 1.37 mm thick, have a straight section of about 480 mm, and they tilt up at a 10° angle in the ends through hard-way bends (i.e. on a plane parallel to the wide side of the cable), with a minimum radius of 349 mm at layer 2. The flared region (ramp) features a straight section of about 125 mm, and is supported by bronze wedges. The expected maximum fields generated by the coils are given in Table I.

III. PRE-LOAD SEQUENCE

The stress in the aluminum shell and rods was monitored with strain gauges during all room-temperature loading operations, cool-downs, and tests. The experimental data are plotted in Figs. 2 and 3, and compared with the results of a 3D finite element model. In the model, shell and rod stresses were optimized to avoid coil-pole separation up to a bore field of 15 T. In Fig. 4, we plotted the peak stress in the coil straight section computed by the model and corresponding to the measured stress values in the shell and rods at room temperature and after cool-down. The

TABLE I
MAGNET PARAMETERS

Parameter	Unit	
Short sample current I_{ss} at 4.3/1.9 K	kA	18.1/20.0
Bore field at 4.3/1.9 K I_{ss}	T	15.6/17.1
Coil peak field at 4.3/1.9 K I_{ss}	T	16.5/18.1
Fx/Fy layer 1 (quadrant) at 18.1 kA	MN/m	+2.5/-0.4
Fz layer 1 (quadrant) at 18.1 kA	kN	100
Fx/Fy layer 2 (quadrant) at 18.1 kA	MN/m	+3.6/-2.4
Fz layer 2 (quadrant) at 18.1 kA	kN	138
Stored energy at 18.1 kA	MJ/m	0.91
Inductance	mH/m	5.6

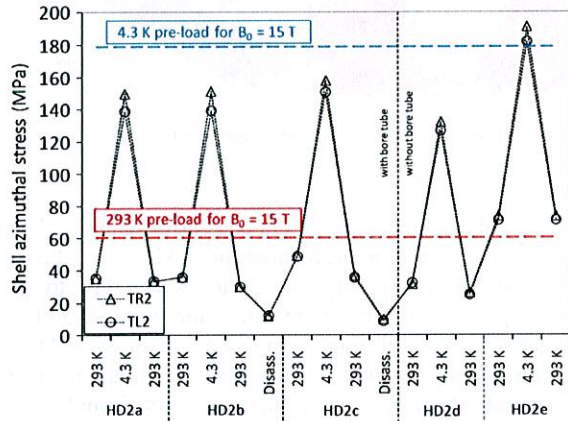


Fig. 2. Azimuthal stress (MPa) of the shell: measured values (markers) and model results (dashed lines) for a 15 T pre-load.

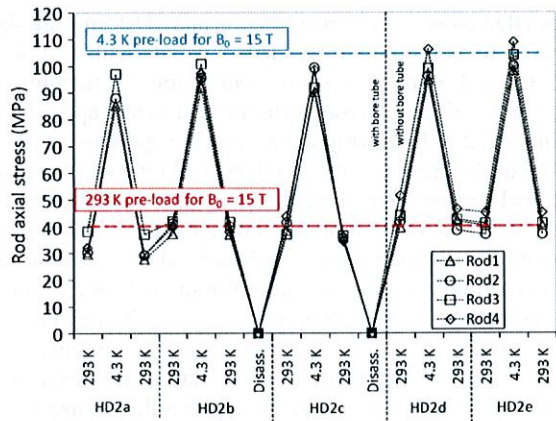


Fig. 3. Axial stress (MPa) of the rods: measured values (markers) and model expectations (dashed lines) for a 15 T pre-load.

peak stress is located in layer 1 pole turn, close to layer 2: because of the round cut-out, the winding pole of layer 1 undergoes an “oval” deformation when pre-load is applied. This causes a compressing stress along the layer 1 pole turn which increases from the mid-plane and peaks in the area close to layer 2.

During the first three tests of the HD2, the shell tension was conservatively maintained at 145–155 MPa, corresponding to a coil peak stress of -135 to -145 MPa. This level of coil pre-load was estimated to ensure no separation up to a bore field of 13.5 T. According to the model, the removal of the bore did not result in a significant change in coil or pole peak stress.

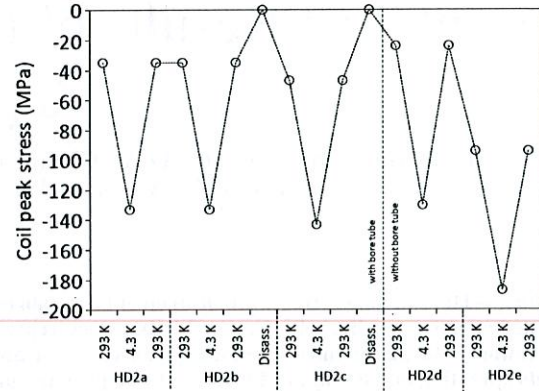


Fig. 4. Computed coil peak stress (MPa) in layer 1 pole turn.

However, a conservative approach was adopted in HD2d and the shell tension was reduced to 130 MPa.

Finally, in the last test, in order to bring the pre-load to a 15 T bore field level, the shell tension was increased to 185 MPa, corresponding to a coil peak stress of -185 MPa. Over the five tests, no significant variation was applied to the rod pre-load, ranging from 90 to 100 MPa at 4.3 K and corresponding to a total axial force of about 550 kN.

IV. TEST RESULTS

A. Training and Ramp-Rate Quenches

In Fig. 5 we plotted the training quenches recorded during all HD2 test (see [2] for the analysis of HD2a-b-c). In the HD2d test, carried out with coil #2 and #3, the removal of the bore tube and the 25 MPa reduction in shell pre-load after cool-down induced a decrease of about 7–8% in quench current during training with respect to HD2c: the magnet started training at a bore field of 9.6 T (59% of I_{ss}) and reached a maximum bore field of 13.4 T (84% of I_{ss}), corresponding to an estimated conductor peak field of 14.1 T, in 46 quenches. In HD2e, the increase in coil pre-load resulted in an additional reduction of about 5–6% in quench current with respect to HD2d: the magnet trained from 8.5 T (52% of I_{ss}) to 12.5 T (74% of I_{ss}) in 43 quenches.

The ramp-rate dependences of the maximum quench currents are plotted in Fig. 6: the increase in current observed in HD2d-e with respect to HD2c, in the range of 35 to 250 A/s, is presently attributed to the improved cooling of the coils achieved by removing the bore tube.

B. Quench Locations

The training quenches were located with the time-of-flight technique using the correlation between I_q/I_{ss} and the velocity v described in [2]. The locations identified in the HD2d-e tests were very consistent with the ones observed in the previous tests: all the quenches were located in the pole turn of layer 1 (Fig. 7, left), despite the 4% lower field with respect to the pole turn in layer 2. In addition, they all occurred in the last 100 mm long regions of the straight section, before the hard-way bend (Fig. 7, right).

The quenches were almost evenly distributed between the two coils, the left and right side of the coil aperture, and, finally, between the lead and return ends. No quenches occurred in the

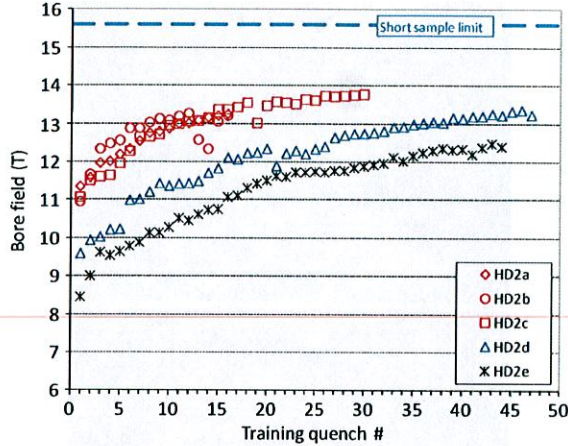


Fig. 5. Bore field (T) as a function of training quenches. The short sample limit of 15.6 T bore field corresponds to a coil peak field of 16.5 T.

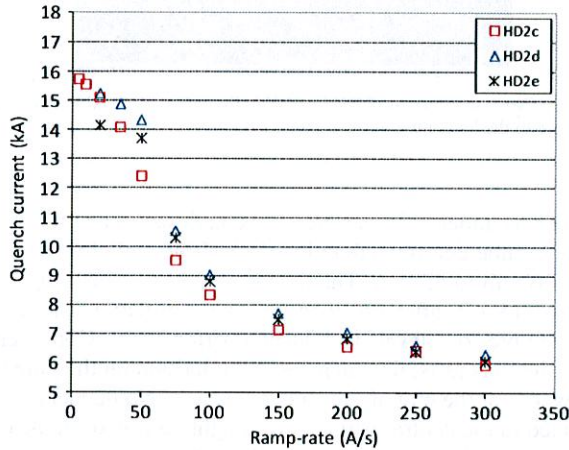


Fig. 6. Maximum quench current (kA) as a function of ramp-rate (A/s).

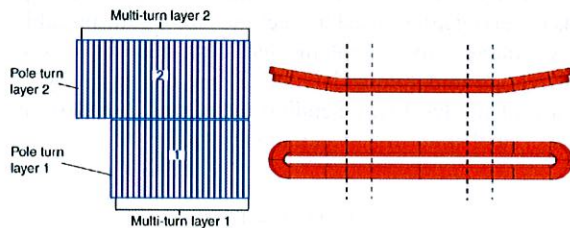


Fig. 7. Left: cross-section of coil layer 1 and layer 2 in the straight section. Right: side and top view of the coil. All the recorded training quenches occurred in the layer 1 pole turn, in the last 100 mm of the straight section, before the hard-way bend (areas comprised between dashed lines).

central part of the straight section or in the end regions (after the hard-way bend).

C. Voltage Signals

In order to identify the possible quench mechanisms limiting HD2 performance, data from voltage taps (Vtaps) were analyzed. The observations made during this analysis were then put into context with expectations from mechanical models and with visual inspections of cross-section cuts of coil #1, where a substantial percentage of quenches occurred in HD2a-b. The first observation made during Vtap data analysis was the lack of

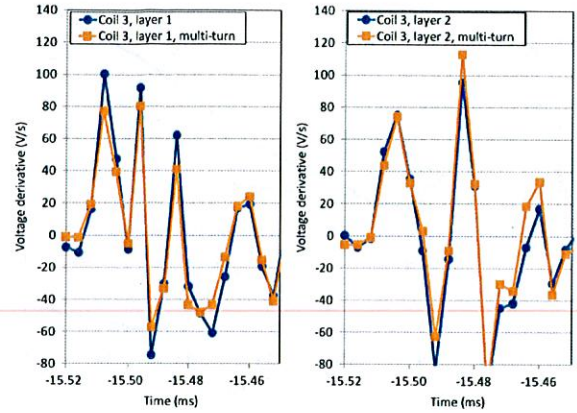


Fig. 8. Voltage derivative signals induced on the inner (left) and outer (right) layers and their multi-turns during a quench in coil #3.

a converging quench-location pattern: as training went on, the location of succeeding quenches shifted almost every time between the four regions indicated in Fig. 7, i.e. in both coils and in all end straight section areas of the layer 1 pole turn.

With the purpose of understanding the slow increase in quench current, we focused our Vtap analysis on the last 20 quenches of HD2e. On the one hand, in order to evaluate the mechanical movements causing the quenches (initial $\sim 100 \mu\text{s}$ since the beginning of the triggering event), we studied the derivative of the voltage induced at the terminals of each layer in both coils. On the other hand, with the purpose of investigating how heat propagated during the quench initiation phase (initial $\sim 10 \text{ ms}$ since the beginning of the triggering event), we looked at the voltage induced across cable sections and across each layer in both coils. This approach is generally considered appropriate because the low frequency components ($< 1 \text{ kHz}$) of the induced voltage is dominated by heat propagation, while the high frequency end ($> 50 \text{ kHz}$) is dominated by mechanical vibrations.

The analyzed HD2e quenches share several characteristics in terms of their onset and heat propagation. In order to find out the location of the slippage triggering the quench, we analyzed the voltage induced on the whole layer and on the multi-turn sector of each layer (Fig. 7, left) at the time of the quench onset in a $\sim 100 \mu\text{s}$ timeframe: the difference between the whole layer and the multi-turn sector provides the signal of the pole turn. Fig. 8 shows an overlap between layer and multi-turn voltage derivatives for inner and outer layer respectively. It can be noticed that an almost simultaneous motion is observed in both layers of coil #3. The excess in the voltage induced in the whole layer 1, compared to the voltage induced in its multi-turn, suggests the presence of a movement of the layer 1 pole turn. Instead, no apparent difference between the signal induced in layer 2 and its multi-turn is observed, indicating a lack of movement of the layer 2 pole-turn. It is important to point out that the observation made above is based on an excess that is just above the noise level. However, this small excess was a recurrent pattern over all the last 20 quenches in HD2e. The consistency in the signal is what gives these small occurrences significance.

Fig. 9 shows the voltage induced in layer 1 and layer 2 of both coils in the 6 ms following the motion discussed above. In this time frame, an increase of voltage can be interpreted as resulting

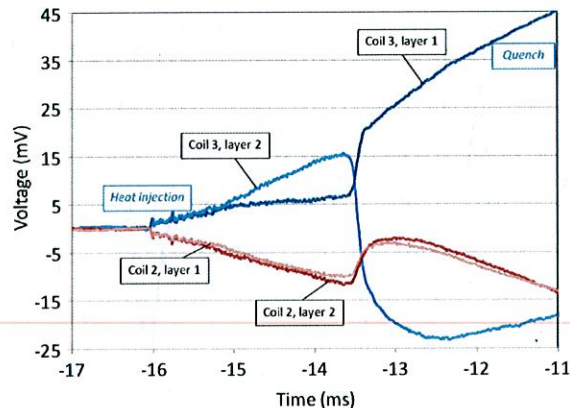


Fig. 9. Voltages signals induced on coil layers during a quench in coil #3.

from heat propagation, which changes the current distribution in the cable and produces a voltage signal. Based on this interpretation, it appears that 1) the heat generated by the onset slippage of Fig. 8 enters both layers of coil #3 at the same time. 2) After a short propagation, heat reaches an additional region in the layer 2. 3) Due to the higher temperature margin, the heat released in layer 2 propagates without inducing a quench. 4) The heat released in layer 1, characterized by lower temperature margin, causes the propagation of a quench.

From the voltage signal analysis made above, we identify the following sequence of events as a possible scenario to explain the last 20 quenches of the HD2e training: a motion occurs in the pole turn of layer 1 and turn 7 of layer 2, close to the upper corner of the layer 1 pole; the heat generated by the slippage propagates in both layers, quenching only layer 1; no motion takes place on the pole turn of layer 2.

D. Coil Visual Inspections

As a way to gather further insight about possible causes of the HD2 training behavior, after the HD2b test coil #1 was cut in correspondence of the center of the straight section (Fig. 10, top picture), where no quenches were recorded, and of the end of the straight section (Fig. 10, bottom picture), where most of the quenches were located.

In the latter, it can be noticed a shift toward the mid-plane of all layer 2 turns after turn 6. The shift determines a compression of the layer 1 turns, and leaves a gap at the top of layer 2. The gap is filled with epoxy, indicating that the turns moved during the winding/reaction process, before impregnation. In addition, the picture points out that turn 7 of layer 2 is partially covering the corner of layer 2 pole. This area coincides with the region where, based on Vtap analysis, quenches were initiated, and, according to the model, the coil peak stress is located.

The vertical displacement of the turns at the end of the straight section appears to be caused by the hard-way bend, which, in the area immediately preceding the end region, pushes the cables towards the mid-plane. In the first 6 turns of layer 2, the effect is prevented by the layer 1 pole.

V. CONCLUSIONS AND NEXT STEPS

After reaching a maximum bore field of 13.8 T, the magnet HD2 was disassembled, reassembled without bore tube, and

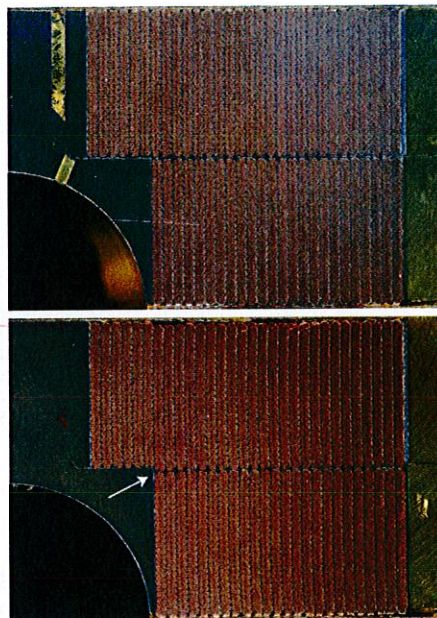


Fig. 10. Cross-section cuts of HD2 coil #1 in the center of straight section (top) and close to the beginning of the hard-way (bottom).

retested as under different pre-load conditions. The removal of the bore tube determined an increase of the coil clear aperture from 36 mm to 43 mm. The magnet reached a maximum bore field of 13.4 T after 46 quenches: no correlation was found between pre-load levels and quench performance. Consistently with previous tests, the quenches were located on the pole turn of layer 1, at the end of the straight section. No quenches were detected in the central part of the straight section or in the ends (after the hard-way bend). The voltage tap signals identified a region between layer 1 and 2 as the area where the quenches were initiated. The analysis was confirmed by cable displacements observed after visual inspection. Among the possible corrective strategies to be implemented in the next set of coils, the following are under consideration: 1) pre-curing of layer 2, 2) increase of the hard-way bending radius and 3) insertion of a stainless steel shim in between the layers.

REFERENCES

- [1] A. F. Lietzke *et al.*, "Test results for HD1, a 16 Tesla Nb₃Sn dipole magnet," *IEEE Trans. Appl. Supercond.*, vol. 14, no. 2, pp. 345–348, Jun. 2004.
- [2] P. Ferracin *et al.*, "Assembly and Test of HD2, a 36 mm bore high field Nb₃Sn dipole magnet," *IEEE Trans. Appl. Supercond.*, vol. 19, no. 3, pp. 1240–1243, Jun. 2009.
- [3] J. Lizarazo *et al.*, "Use of high resolution DAQ system to aid diagnosis of HD2b, a high field Nb₃Sn dipole," presented at the Applied Superconductivity Conference, Chicago, IL, USA, August 17–22, 2008.
- [4] X. Wang *et al.*, "Magnetic field measurements of HD2, a high field Nb₃Sn dipole magnet," presented at the Particle Accelerator Conference, Vancouver, Canada, May 4–8, 2009.
- [5] G. Sabbi *et al.*, "Design of HD2: A 15 T Nb₃Sn dipole with a 35 mm bore," *IEEE Trans. Appl. Supercond.*, vol. 15, no. 2, pp. 1128–1131, Jun. 2005.
- [6] P. Ferracin *et al.*, "Mechanical design of HD2, a 15 T Nb₃Sn dipole magnet with a 35 mm bore," *IEEE Trans. Appl. Supercond.*, vol. 16, no. 2, pp. 378–381, Jun. 2006.
- [7] P. Ferracin *et al.*, "Development of the 15 T Nb₃Sn Dipole HD2," *IEEE Trans. Appl. Supercond.*, vol. 18, no. 2, pp. 277–280, Jun. 2008.